ACS OMEGA

http://pubs.acs.org/journal/acsodf

Article

Is Cys(MTSL) the Best α-Amino Acid Residue to Electron Spin Labeling of Synthetically Accessible Peptide Molecules with Nitroxides?

Barbara Biondi,* Victoria N. Syryamina,* Gabriele Rocchio, Antonio Barbon, Fernando Formaggio, Claudio Toniolo, Jan Raap, and Sergei A. Dzuba

Cite This: *ACS Omega* 2022, 7, 5154−5165

Read Online

ACCESS | Metrics & More | Article Recommendations | Supporting Information

ABSTRACT: Electron paramagnetic resonance spectroscopy, particularly its pulse technique double electron−electron resonance (DEER) (also termed PELDOR), is rapidly becoming an extremely useful tool for the experimental determination of side chain-to-side chain distances between free radicals in molecules fundamental for life, such as polypeptides. Among appropriate probes, the most popular are undoubtedly nitroxide electron spin labels. In this context, suitable biosynthetically derived, helical regions of proteins, along with synthetic peptides with amphiphilic properties and antibacterial activities, are the most extensively investigated compounds. A strict requirement for a precise distance measurement has been identified in a minimal dynamic flexibility of the two nitroxide-bearing α-amino acid side chains. To this end, in this study, we have experimentally compared in detail the side-chain mobility properties of the two currently most widely utilized residues, namely, Cys(MTSL) and 2,2,6,6-tetramethylpiperidine-1-oxyl-4-amino-4-carboxylic acid (TOAC). In particular, two double-labeled, chemically synthesized 20-mer peptide molecules have been adopted as appropriate templates for our investigation on the determination of the model intramolecular separations. These double-Cys(MTSL) and double-TOAC compounds are both analogues of the almost completely rigid backbone peptide ruler which we have envisaged and 3D structurally analyzed as our original, unlabeled compound. Here, we have clearly found that the TOAC side-chain labels are largely more 3D structurally restricted than the MTSL labels. From this result, we conclude that the TOAC residue offers more precise information than the Cys(MTSL) residue on the side chain-to-side chain distance distribution in synthetically accessible peptide molecules.

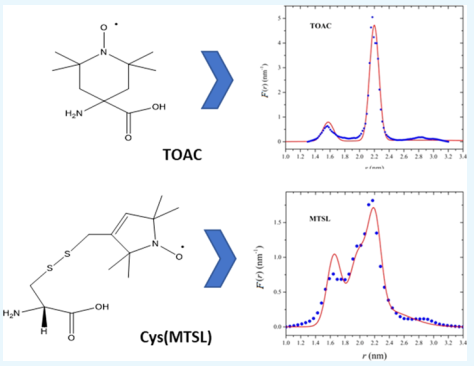

INTRODUCTION

Proteins and polynucleotides are the fundamental molecules of life. Interestingly, they are composed of a limited number of monomer types, the succession of which in the main chain determines their function. This later, in turn, is strictly dependent on the 3D structure adopted by the biomolecule. Therefore, studying the conformation of these molecules is of primary relevance. To this aim, nuclear magnetic resonance (NMR), circular dichroism (CD), X-ray diffraction crystallography, and fluorescence are undoubtedly among the most widely exploited techniques for solution- and crystal-state investigations. However, interest for electron paramagnetic resonance (EPR) is steadily increasing because this spectroscopy can be used in a variety of environments, and in addition, it relies on highly specific probes. In particular, pulsed EPR experiments, such as double electron−electron resonance[1−4] (DEER, also known as PELDOR, i.e., pulsed electron double resonance), allow for measuring distances between paramagnetic probes, spaced from almost 20 to 160 Å (in the latter case, in deuterated compounds).[5] This opportunity permits one to obtain information on the 3D structure of a macromolecule, on the formation of aggregates, and on interactions among different types of molecules.

In this context, nitroxide electron spin labels are by far the most used probes. They were utilized for seminal measurements of distances in isolated proteins[6−14] and within cells[15−17] for analyzing conformational transitions of the prion protein,[18] for unraveling DNA mechanisms,[19−21] for investigating conformation, aggregation, and membrane interactions of peptaibols,[22−27] for studying peptide distribution and mobility on solid supports,[28,29] for understanding host−guest interactions in supramolecular chemistry,[30] and more recently for examining proteins of interest to food science.[31] In any case, here it is fair to mention that in recent years, additional promising approaches different from nitro-

Received: November 5, 2021
Accepted: December 27, 2021
Published: January 31, 2022

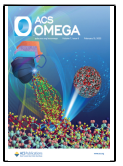

ACS Publications

© 2022 The Authors. Published by American Chemical Society

xides have been utilized for assessing distances between free radical moieties in proteins [e.g., lanthanide (Gd^{3+}) tags,[32] double His-Cu^{2+}-based labels,[33] and trityl (triarylmethyl)-based labels[34,35]].

Two very popular nitroxide probes in peptide/protein (including protein peptidic fragments) investigations are the C^{α}-tetrasubstituted α-amino acid TOAC (2,2,6,6-tetramethylpiperidine-1-oxyl-4-amino-4-carboxylic acid)[36−41] (Figure 1)

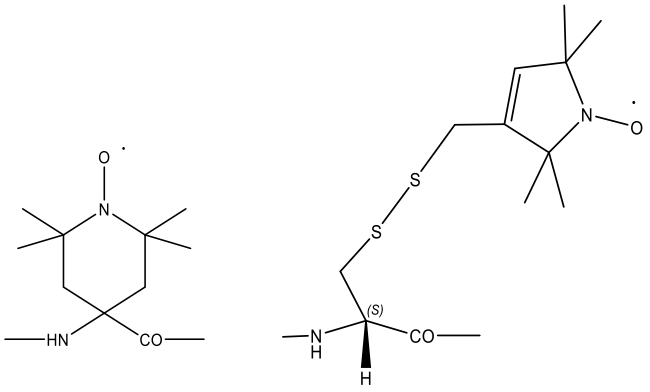

Figure 1. Chemical structures of the TOAC (left) and L-Cys(MTSL) (right) electron spin-labeled α-amino acid residues.

and MTSL (methanethiosulfonate spin labels; 1-oxyl-2,2,5,5-tetramethylpyrroline-3-methyl) nitroxide[42] selectively reacts with the side-chain thiol group of the coded Cys residue to generate Cys(MTSL) (Figure 1).

Unfortunately, the Cys(MTSL) spin probe is able to explore a relatively wide conformational space as it is connected to the peptide backbone through as many as five rotatable σ-bonds, although interconversions between some of the various states might be too slow to contribute significantly to the overall nitroxide motions.[13] In addition, the presence of a relatively rare Cys residue is required in a natural peptide/protein (or alternatively, it should be biosynthetically incorporated). To overcome, at least in part, these latter limitations, a few other coded amino acid-based electron spin probes were proposed, but also in these cases, various σ-bonds separate the nitroxide moiety from the peptide main chain.[9−12,43] Also, a slightly less flexible arm is sometime provided when the Cys side chain is functionalized with shorter substituents.[44] In any case, the conformational restriction characteristic of TOAC is unique, superior to that of any side-chain functionalized, coded amino acid electron spin probe. Actually, its paramagnetic group is tightly bound to the peptide backbone through a six-membered ring group. Thus, TOAC offers an essential advantage for distance measurements in view of its precise spatial location and quasi-rigid nitroxide orientation.[45]

Another favorable property of TOAC is the possibility to insert it by chemical synthesis, although by a careful, usually nonroutine solid-phase procedure,[38,39,41] at any position of a polypeptide chain. Nevertheless, it is evident that this replacement is appropriate if in that region of the original sequence a helical segment is already present because TOAC is well known to be a helix inducer (and a β-sheet breaker).[46−48] Moreover, it should be admitted that the noncoded TOAC has so far escaped all attempts to be biosynthetically incorporated in any polypeptide molecule. By contrast, the corresponding properties of Cys are (i) easy insertion in a growing peptide chain by chemical synthesis using a suitable side-chain protected derivative and (ii) its only weak conformational bias in favor of the β-sheet structure and in the destabilization of the α-helix.[49]

To experimentally prove the different properties of the TOAC and Cys-functionalized electron spin probes and to highlight the uncertainty in the distance determination when using the latter, in this work we chemically synthesized and spectroscopically compared two α-helical peptides, one containing two TOAC residues, separated by four helix turns, and the second characterized by two Cys(MTSL) replacing the two TOAC.

RESULTS AND DISCUSSION

Design of the Doubly Electron Spin-Labeled α-Helical Peptides. A proper distance between two nitroxyl radicals in a DEER investigation is in the range 20−25 Å. In this study, our target was a peptide system in α-helical conformation. In a regular α-helix, each turn comprises 3.6 residues, and seven amino acids are necessary to obtain two side chains precisely on top of one another at a distance of 11 Å. To achieve a distance between the two nitroxyl probes appropriate for the EPR investigation, a separation of 14 residues between the labels is required. Considering this parameter and that in a stable α-helix at least two residues both at the N- and C-termini are considered rather mobile, at least 20 residues should occur to obtain a quasi-rigid backbone ruler to be used for the EPR investigation. On this basis, we designed an N-acetylated (Ac) 20-mer model peptide amide (peptide **I** in Table 1) characterized by an alternation of the helicogenic C^{α}-tetrasubstituted α-aminoisobutyric acid (Aib)[50,51] and two of the most helicogenic protein amino acids, Ala and Lys.[49] To evaluate the reliability of different electron spin labels in distance measurements, we designed and synthesized, in addition to the unlabeled peptide (**I**), two analogues (**II** and **III**), all with a well-defined, Aib-generated, stable α-helical structure. For our investigation, we selected two different nitroxyl probes with different conformational stabilities, the helicogenic TOAC residue and the *S*-(1-oxyl-2,2,5,5-tetramethyl-2,5-dihydro-1*H*-pyrrol-3-yl)methyl (MTSL) group covalently linked to the side chains of the Cys residues in sequence. In the TOAC-containing peptide, analogue **II**, we introduced its electron spin label at positions 3 and 17 ($i \rightarrow i + 14$) where the helix-promoting Aib residues of the same C^{α}-tetrasubstituted class were present in the original model peptide. The MTSL electron spin probe reagent needs to be conjugated with two Cys in sequence without perturbing the overall helical conformation of the peptide. To this aim, we decided to insert the Cys residues at positions 4 and 18 ($i \rightarrow i$

Table 1. Peptide Sequences

	peptide squence	
Ac-20-NH_2	Ac-Aib-Lys-Aib-Ala-(Aib-Lys-Aib-Ala)$_3$-Aib-Ala-Aib-Lys-NH_2	**I**
Ac-[$TOAC^{3,17}$]-20-NH_2	Ac-Aib-Lys-**TOAC**-Ala-(Aib-Lys-Aib-Ala)$_3$-**TOAC**-Ala-Aib-Lys-NH_2	**II**
Ac-[$Cys(MTSL)^{4,18}$]-20-NH_2	Ac-Aib-Lys-Aib-Cys(**MSTL**)-(Aib-Lys-Aib-Ala)$_3$-Aib-Cys(**MSTL**)-Aib-Lys-NH_2	**III**

https://doi.org/10.1021/acsomega.1c06227
ACS Omega 2022, 7, 5154−5165

+ 14) (peptide **III**), thus maintaining the presence of the helix-promoting Aib amino acids.

Peptide Synthesis and Characterization. Solid-phase peptide synthesis (SPPS) protocols were used for the difficult syntheses of the unlabeled sequence **I** and the two differently double-labeled analogues. The high content of C^{α}-tetrasubstituted α-amino acids (50% Aib and/or TOAC in sequence) required the optimization of a protocol able to overcome the low reactivity of the N^{α}-amino group of those two residues. In all of the syntheses, we employed [*O*-(7-azabenzotriazol-1-yl)-1,1,3,3-tetramethyluronium hexafluorophosphate][52] as the C-activation method and repeated each peptide coupling reaction twice.[53]

The synthesis of the TOAC-labeled analogue proved to be the most difficult. Besides the difficulties involving the introduction of the electron spin-labeled amino acid, the nitroxyl group is particularly sensitive to the strong acidic conditions used in the cleavage and purification steps which convert the free radical to its N-hydroxylated species.[54] To completely recover the nitroxyl radical character, an alkaline treatment with 1 M ammonium hydroxide for 180 min was required. The reaction was checked by HPLC analysis. The crude peptide was purified by preparative HPLC, thus avoiding the presence of the acidic modifier trifluoroacetic acid in the elution system.

The conjugation of the MTSL electron spin reagent on the Cys-containing peptide was performed in solution. Once synthesized by SPPS, the peptide was cleaved from the resin in the presence of a proper scavenger to avoid formation of the disulfide bond and then subjected to a preliminary purification step. For the functionalization step, the side-chain free Cys containing peptide was dissolved in a buffer solution in an argon atmosphere and treated with an excess of the MTSL spin reagent. The reaction was monitored by HPLC, and the lyophilized crude peptide was purified by preparative HPLC.

For all samples, the correctness of the chemical assignments to the peptide fractions obtained by HPLC purification was confirmed by HPLC-MS analyses (Table S2, Supporting Information).

Conformational Analysis. The preferred conformations of the unlabeled, terminally blocked peptide Ac-20-NH_2 (**I**) and its two nitroxyl-labeled analogues Ac-[$TOAC^{3,17}$]-20-NH_2 (**II**) and Ac-[$Cys(MTSL)^{4,18}$]-20-NH_2 (**III**) were investigated in solvents of diverging polarities and at different concentrations by the use of Fourier transform infrared (FT-IR) absorption, electronic CD, and 2D NMR.

The FT-IR absorption spectra in a solvent of limited polarity ($CDCl_3$) were obtained in the N−H stretching (3450−3200 cm^{-1}) and C═O stretching (1750−1600 cm^{-1}) regions. In all three compounds at 1 mM peptide concentration, very intense absorption bands are seen with maxima at 3306−3309 cm^{-1} (Figure 2) and near 1659 cm^{-1}, respectively. We attribute these peaks to the N−H and C═O vibrators of strongly H-bonded amide/peptide groups. The typical corresponding bands for intramolecularly H-bonded, peptide helical structures are close, being seen at approximately 3330 and 1655 cm^{-1}.[55,56] The absence of self-aggregation in the stabilization of this peptide conformation is indicated by the remarkable spectral consistency upon peptide dilution to 0.1 mM concentration (not shown). An extremely weak band near 3420 cm^{-1}, assignable to solvated N−H vibrators of the N-terminal peptide groups not part of the intramolecular H-bonding scheme, is hardly visible in the spectra (Figure 2).

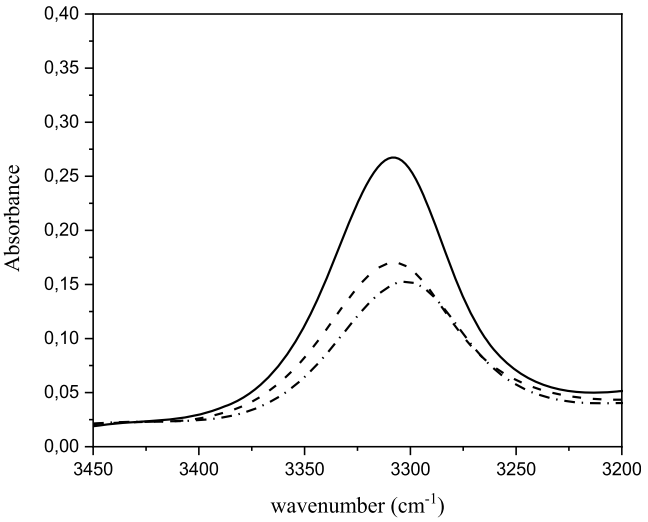

Figure 2. FT-IR absorption spectra in the N−H stretching region of the Ac-20-NH_2 (solid line), Ac-[$TOAC^{3,17}$]-20-NH_2 (dashed line), and Ac-[$Cys(MTSL)^{4,18}$]-20-NH_2 (dashed-dotted line) peptides in $CDCl_3$ solution at 1 mM concentration.

From this spectroscopic analysis, we conclude that in $CDCl_3$ solution, the largely prevailing conformation of the three unassociated 20-mer peptides, with 50% proportion of the helicogenic C^{α}-tetrasubstituted α-amino acids Aib[50,51] and TOAC,[41,57] is remarkably folded and stabilized by intramolecular C═O···H−N H-bonds.

The far-UV CD curves of the three peptides in methanol (MeOH) (Figure 3, left) are quite comparable in shape, but the intensities of the TOAC-containing analogue are different (although slightly). They exhibit two strong negative bands located near 208 and 225 nm, accompanied by an even stronger positive band at about 192 nm, typical of the $n \rightarrow \pi^*$ transition and of the parallel/perpendicular components of the split $\pi \rightarrow \pi^*$ transition of the amide chromophores, respectively, in right-handed helical peptides.[58,59] Interestingly, the side-chain nitroxyl chromophores of the two Cys(MTSL) residues do not seem to contribute at all in this spectral region, whereas those of the two TOAC residues appear to provide a limited effect.[60] The R, $[\theta]_{222}/[\theta]_{208}$, values indicative of the type of helical structure adopted[58,59,61] are 0.8 and 0.9 for all three peptides, clearly suggesting that the α-helix conformation is largely preferred over the 3_{10}-helix. This finding is not surprising, considering the relevant backbone length (20 amino acids) of these peptides.[61] From the comparison of these three curves with those in H_2O solution (Figure 3, right), it is clear that the intensities and, consequently, the related peptide structurations are remarkably lower in an aqueous environment (but the α-helix component is still always prevailing, with *R* values 0.8−1.1).

The near-UV/visible CD curves of the two nitroxyl-labeled peptides (Figure 4) diverge dramatically. The *bis*-TOAC labeled analogue shows an intense maximum at 422 nm, arising from the nitroxyl chromophore $n \rightarrow \pi^*$ transition of the achiral amino acid. This positive, induced CD band is brought about by the right-handed helical structure of the host peptide, in analogy with the observations already reported for similar compounds.[41,60,62]

This type of evidence confirms the structuration of the peptide. Conversely, the CD curve for the *bis*-Cys(MTSL) analogue is significantly weaker in the same spectral region.

https://doi.org/10.1021/acsomega.1c06227
ACS Omega 2022, 7, 5154−5165

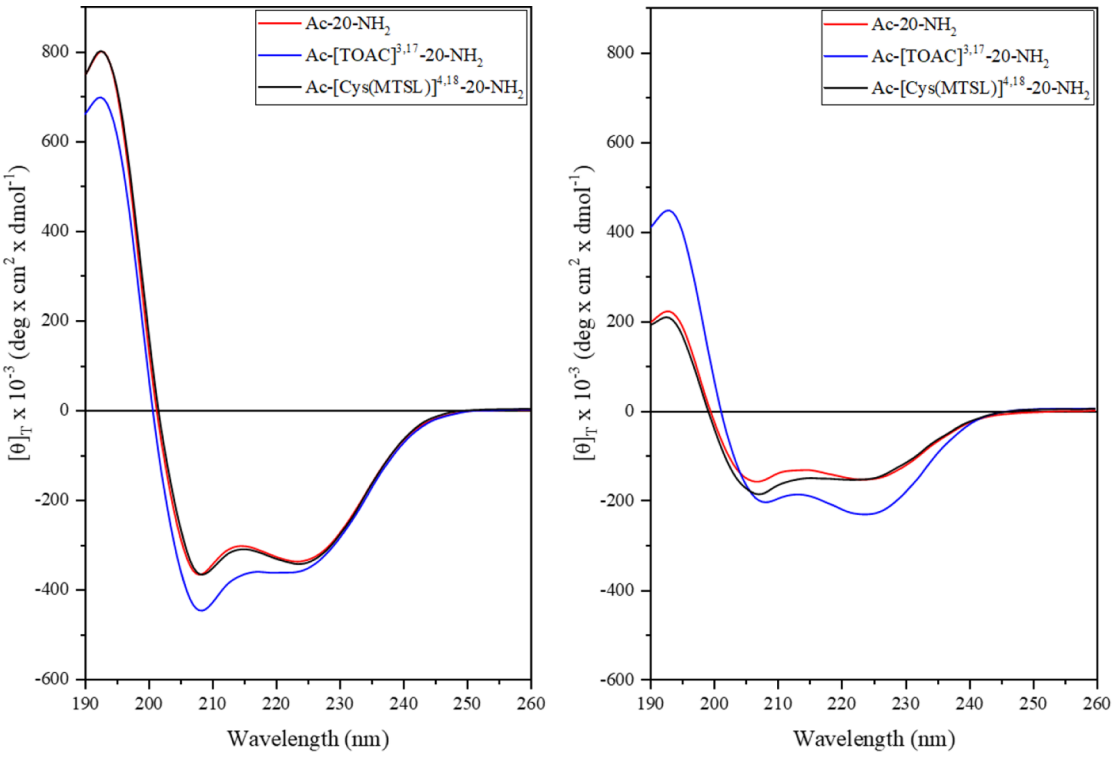

Figure 3. Far-UV CD spectra of the three compounds studied in MeOH (left) and water solutions (right) (peptide concentration: 0.3 mM).

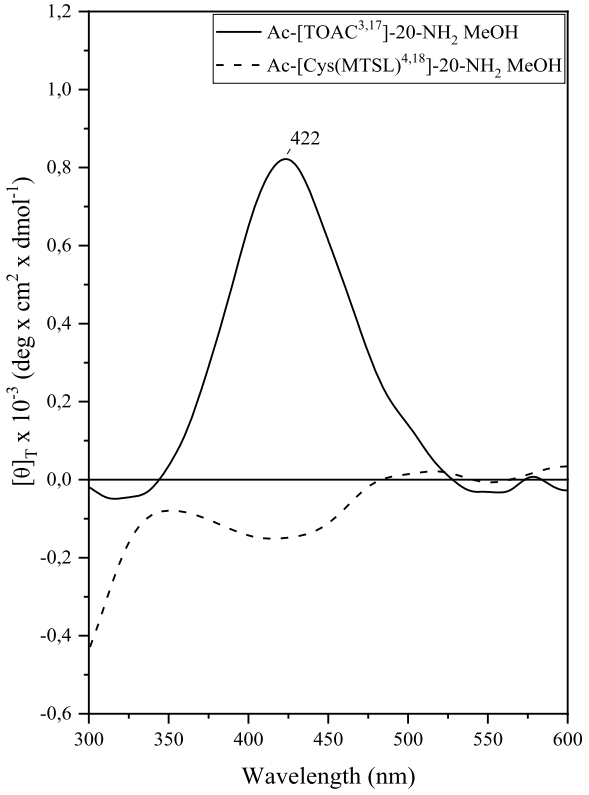

Figure 4. Near-UV and visible spectra of the two nitroxyl-labeled compounds studied in MeOH solution (peptide concentration: 1 mM).

This result supports our view that the MTSL nitroxide is covalently attached not only quite far from the source of the chirospectroscopic effect (the peptide backbone) but also via a mobile side chain.[63,64] More information about this type of mobility has been obtained by continuous-wave EPR (CW-EPR) (see below). Therefore, it is reasonable that its CD intensity would be only marginally influenced by the helical peptide chirality.

The 2D NMR investigation allowed us to obtain more detailed information on the 3D structural preferences of the unlabeled Ac-20-NH_2 peptide in MeOH, d_3 solution. The C−H and N−H peaks were attributed on the basis of the Wüthrich methodology.[65] The complete assignment of the proton resonances is shown in the Supporting Information (Table S3). Since it is well known that a limitation in the physicochemical analyses of −N−O· containing compounds is that most of the proton resonances in their ^{1}H NMR spectra are remarkably broadened owing to the paramagnetic effect induced by the nitroxyl radical, we did not make any attempt to characterize either the Ac-[$TOAC^{3,17}$]-20-NH_2 analogue or its $Cys(MTSL)^{4,18}$ counterpart by 2D NMR.

From the presence of all of the $NH_i \rightarrow NH_{i+1}$ sequential cross peaks, the nuclear Overhauser effect spectroscopy (NOESY) spectrum of the unlabeled 20-mer, terminally blocked, peptide shown in Figure 5 represents an unambiguous proof that this compound is completely folded in a helical structure. This finding is in line with our conformational conclusions on the same compound obtained by FT-IR absorption and CD spectroscopies discussed above. In the NOESY fingerprint region. we noted multiple $C^{\alpha/\beta}H_i \rightarrow NH_{i+3}$ correlations and, more interestingly, one $C^{\alpha/\beta}H_i \rightarrow NH_{i+4}$ typical of the α-helical structure [for that involving $C^{\beta}H_i \rightarrow NH_{i+4}$; see Figure 6]. It is relevant that the $C^{\alpha}H_i \rightarrow NH_{i+2}$ interactions, indicative of the 3_{10}-helix, seem to be absent. A summary of all significant interresidue NOESY cross peaks for Ac-20-NH_2 is given in Figure 7.

Based on the α-helical propensity of the two labeled peptides, we proceeded to generate the corresponding PyMOL

https://doi.org/10.1021/acsomega.1c06227
ACS Omega 2022, 7, 5154−5165

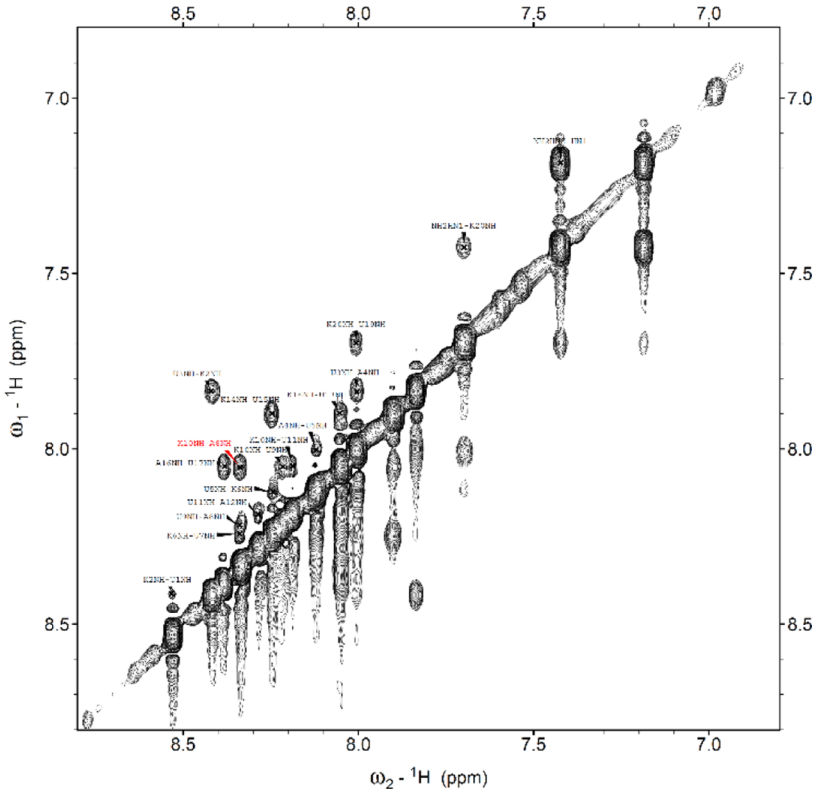

Figure 5. Amide NH proton region of the NOESY spectrum of the Ac-20-NH_2 peptide in MeOH, d_3 solution at 2 mM concentration. The $NH_i \rightarrow NH_{i+1}$ cross peaks are marked in black.

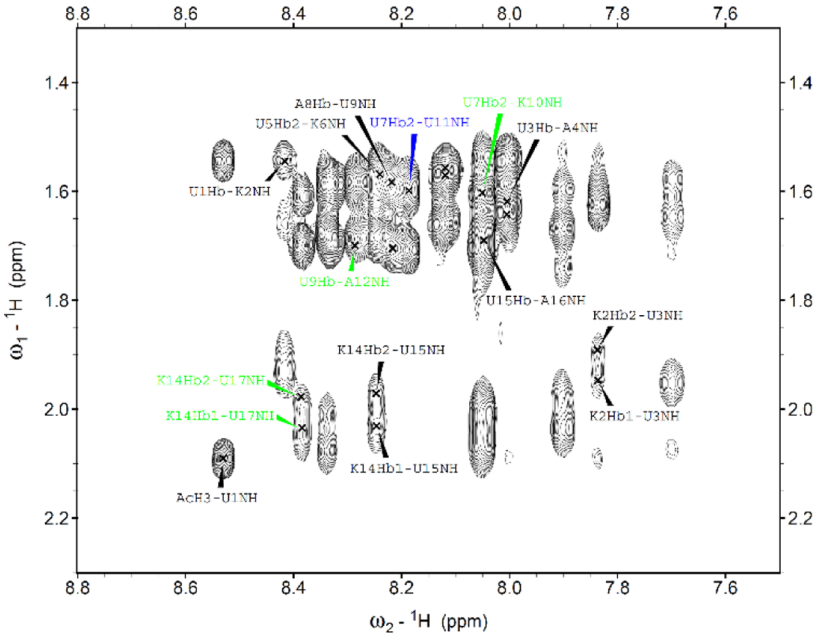

Figure 6. Region of the NOESY spectrum of the Ac-20-NH_2 peptide in MeOH, d_3 solution at 2 mM concentration. The $C^{\beta}H_i \rightarrow NH_{i+4}$ cross peak is marked in blue.

3D model to highlight the relative position of the nitroxyl labels. From these amino acid sequences, it is clear that in each labeled peptide, the two nitroxyl building blocks were by purpose separated by 14 residues, consistent with four complete turns of the α-helix. Therefore, we were not surprised to find the two nitroxyl moieties located on the same side of the α-helix (Figures 8 and 9). In addition, from the 3D models, we were able to extrapolate the distance between the two TOAC in the Ac-[$TOAC^{3,17}$]-20-NH_2 peptide and that between the two Cys(MTSL) residues in the Ac-[$Cys(MTSL)^{4,18}$]-20-NH_2 peptide. In particular, the distances between the two nitroxyl oxygen atoms in each of the two compounds (25.6 and 22.9 Å, respectively) will allow a

https://doi.org/10.1021/acsomega.1c06227
ACS Omega 2022, 7, 5154−5165

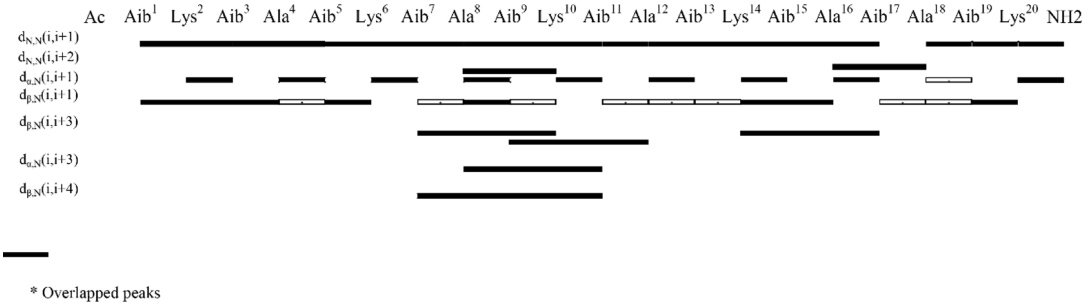

Figure 7. Summary of the significant interresidue NOESY cross peaks for the Ac-20-NH_2 peptide in MeOH, d_3 solution at 2 mM concentration.

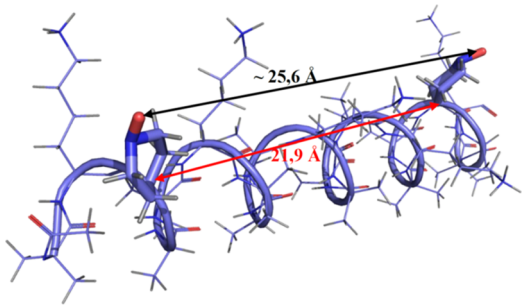

Figure 8. 3D model of the Ac-[$TOAC^{3,17}$]-20-NH_2 peptide in the α-helical conformation obtained using PyMOL software. The distance between the C^{α}-atoms (red arrow) and between the nitroxyl oxygen atoms (black arrows) of the two TOAC residues are measured from the model itself.

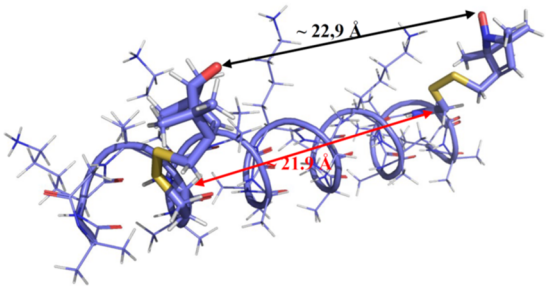

Figure 9. 3D model of the Ac-[$Cys(MTSL)^{4,18}$]-20-NH_2 peptide in the α-helical conformation obtained using PyMOL software. The distance between the C^{α}-atoms (red arrow) and between the nitroxyl oxygen atoms (black arrows) of the two Cys(MTSL) residues are measured from the model itself.

direct comparison with the corresponding data available from the EPR (DEER) experiments discussed below.

EPR Study. The room-temperature CW-EPR spectra in *fluid* solution of the synthetic compounds Ac-[$TOAC^{3,17}$]-20-NH_2 and Ac-[$Cys(MTSL)^{4,18}$]-20-NH_2 confirm the presence of the radical nitroxide attached to the chemical structures: the spectra are characterized by relatively broad lines, especially for the TOAC-labeled system (Supporting Information), consistent with its large molecular dimension.[42] While for the TOAC rigid system, the reorientational motion is due to that of the whole molecule, the narrower linewidth of the Cys(MTSL)-labeled compound makes us to assume that the MTSL probe would undergo a local mobility because of the flexibility of the peptide···radical linker chain.

The CW-EPR spectra for the two TOAC- and MTSL-labeled peptides obtained at *100 K* are reported in Figure 10A along with the simulations performed using EasySpin software.

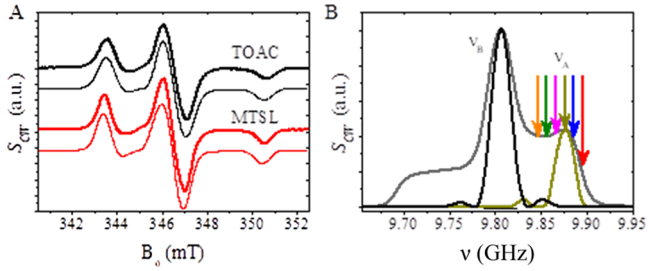

Figure 10. (A) CW-EPR spectra at 100 K for the TOAC- and MTSL-labeled peptides (thick lines are the experimental spectra, thin lines are the best fits). (B) Echo-detected EPR spectrum of the TOAC-labeled peptide at 80 K in the frequency domain. The black curve shows the excitation profile of the pumping pulse, and the colored arrows show the echo detected positions in the DEER measurements.

The EPR line shape is characteristic for immobilized nitroxide labels without pronounced broadening of the individual line width due to the dipole−dipole interaction. The best fitted g- and hyperfine A principle tensor values were found as g_{TOAC} = [2.0129 2.0107 2.0065], A_{TOAC} = [15.5 15.5 97.8] MHz, and g_{MTSL} = [2.0141 2.0098 2.0067], A_{MTSL} = [13.7 13.7 98.5] MHz.

Since the expected spin···spin distance is about 2.2 nm[66] (14 residues for an α-helical peptide), CW-EPR spectroscopy is insensitive to the spin···spin distance evaluation. This distance range is meanwhile typical for detection in the DEER experiments.[67,68] The obtained DEER time traces are presented in Figure 11 in a normalized form [eq 1, see below]. The original DEER time traces are shown in Figure S8. To explore the effect known as orientational selectivity,[69−72] the DEER time traces in Figure 11 are acquired at different frequency offsets from the pumping pulse position.

In Figure 11A, one can see that, for the case of the TOAC-labeled peptide, the data strongly depend on the frequency offset, while for the MTSL-labeled peptide, the orientational effect is much less pronounced (Figure 11B). The Fourier transforms of the DEER time traces are illustrated in Figure 11C,D for the TOAC- and MTSL-labeled peptides, respectively. For the TOAC-labeled peptide, the dependence is also strongly pronounced. Suppression of the canonical dipolar orientations, either in the perpendicular orientations (Pake "horns") or in the parallel orientations (Pake "shoulders"), is clearly visible. However, for the MTSL-labeled peptide, the frequency-domain data are nearly independent of the frequency offset.

As eq 2 is valid for randomly distributed orientations, the determination of the pair spin···spin distribution function $F(r)$ from eq 2 was performed by employing the averaged DEER

https://doi.org/10.1021/acsomega.1c06227
ACS Omega 2022, 7, 5154−5165

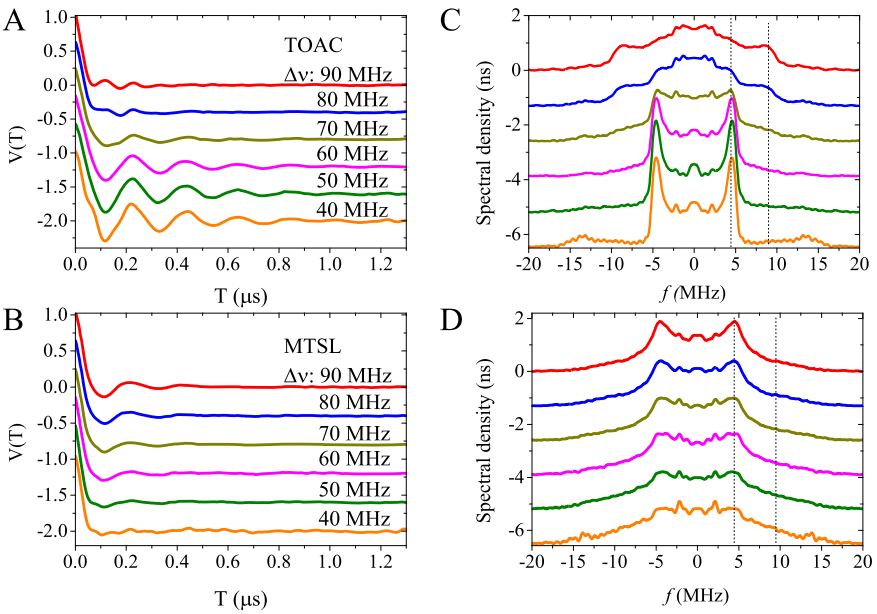

Figure 11. Normalized DEER traces for the TOAC- (A) and MTSL-labeled (B) peptides at different frequency offsets. The curves are shifted downward for convenience. (C,D) Corresponding Fourier transforms for TOAC- (C) and MTSL-labeled (D) peptides. The colors are the same as in panels (A,C). The curves are shifted downward for convenience. The vertical dotted lines show canonical orientations in the Pake-pattern.

time traces and the corresponding Fourier transforms (Figure 12, left panels). The DEER traces at 90−40 MHz offsets were summed with a weighting function, accounted as an echo signal intensity at the detection position in the EPR spectrum. The experimental distance distributions $F(r)$ for both peptides are shown in Figure 12 (right panels). For both cases, the $F(r)$ functions attain their maxima at r = 2.19 nm. However, the shape of the distributions is quite different: for the TOAC-labeled peptide, it is a single narrow line, while for the MTSL-labeled peptide, the line is much broader, with an additional maximum appearing near 1.95 nm.

Most probably, this distribution broadening for the MTSL-labeled peptide points to the presence of several conformers (at least two of them). As this broadening is not observed for the TOAC-labeled peptide, certainly these conformers are not intrinsic to the unlabeled peptide but are induced by the flexibility of the MTSL linker (Figure 1).

Note that the small peaks in the frequency domain located at 13.6 and 2.4 MHz (insets to Figure 12) are caused by contamination of the ^{1}H and ^{2}H electron spin echo envelope modulation (ESEEM) signals, which arise from partial overlapping of the pumping and detection pulses and are more pronounced at smaller frequency offsets, as also seen in Figure 11C,D. As the three-pulse DEER experimental setup was used,[4] which does not assume an averaging scheme as it is in the four-pulse DEER setup, to exclude these artificial lines in the dipolar spectrum, one is forced to use large frequency offsets between the detection and pumping pulses. We probed the detection on the low-frequency shoulder of the EPR spectrum (Figure 10B) with a 112 MHz offset of the pumping pulse. The data shown in Figure S9 were found to be free of these peaks, confirming the electron-nucleus coupling manifestation in the frequency spectra in Figure 11C,D. These peaks result in artifacts appearing in the $F(r)$ distribution function near 1.6 and 2.9 nm for both peptides (Figure 12, right panels).

This newly observed impact of orientational selectivity for TOAC DEER,[69−72] reflected in Figure 11, invites the researchers who plan to incorporate this labeled amino acid in polypeptide molecules to select their templates accurately.

Moreover, this effect allows assessing the mutual orientation of the principal axis system and the vector connecting the two spin labels (dipolar vector). For the double-labeled molecules at X-band, this effect has already been explored.[70,71] We found that our data resemble those reported for the case where the spin labels are rigidly attached to DNA fairly well.[70] Indeed, in our case, for the expected α-helix, the dipolar vector between the TOAC^{3} and TOAC^{17} spin labels in the nitroxide molecular frame is almost parallel to the peptide helix (Figure 8). Thus, for the case of detection at $\Delta\nu \approx 40$ MHz (the detection at the equatorial orientation of the magnetic field in the nitroxide molecular framework), the Pake "horns" satisfy approximately the condition of the perpendicular orientation of the dipolar vector; meanwhile, the appearance of Pake "shoulders" at detection $\Delta\nu \approx 90$ MHz (the detection at the axial orientation of the magnetic field) requires the dipolar angle to be $\theta \approx 0°$ (the evaluation of the dipolar angle at different probed orientations is shown in Supporting Information, Figures S10 and S11). Thus, we conclude that our results may be explained if we assume two labels having nearly parallel directions for the axial axes, with the dipolar axis only slightly deviating from this direction caused by the slight difference of TOAC^{3} and TOAC^{17} positions due to two turns of α-helix, as shown in Figure 8. Therefore, the observed orientational selectivity effects for the TOAC-labeled peptide are close to the case of DNA I in ref 68. More accurate data analysis could be carried out by use of molecular modeling.

In summary, our DEER data for the TOAC-labeled peptide indicate a much narrower distance distribution as compared with that of the MTSL-labeled peptide. In the latter case, the experimental distance distribution possesses additional maxima which unambiguously point to the existence of at least two labeled conformers. It is known that one nitroxide label may occupy several distinct regions of the conformational space.[73,74] Thus, TOAC labels are much more rigid than

https://doi.org/10.1021/acsomega.1c06227
ACS Omega 2022, 7, 5154−5165

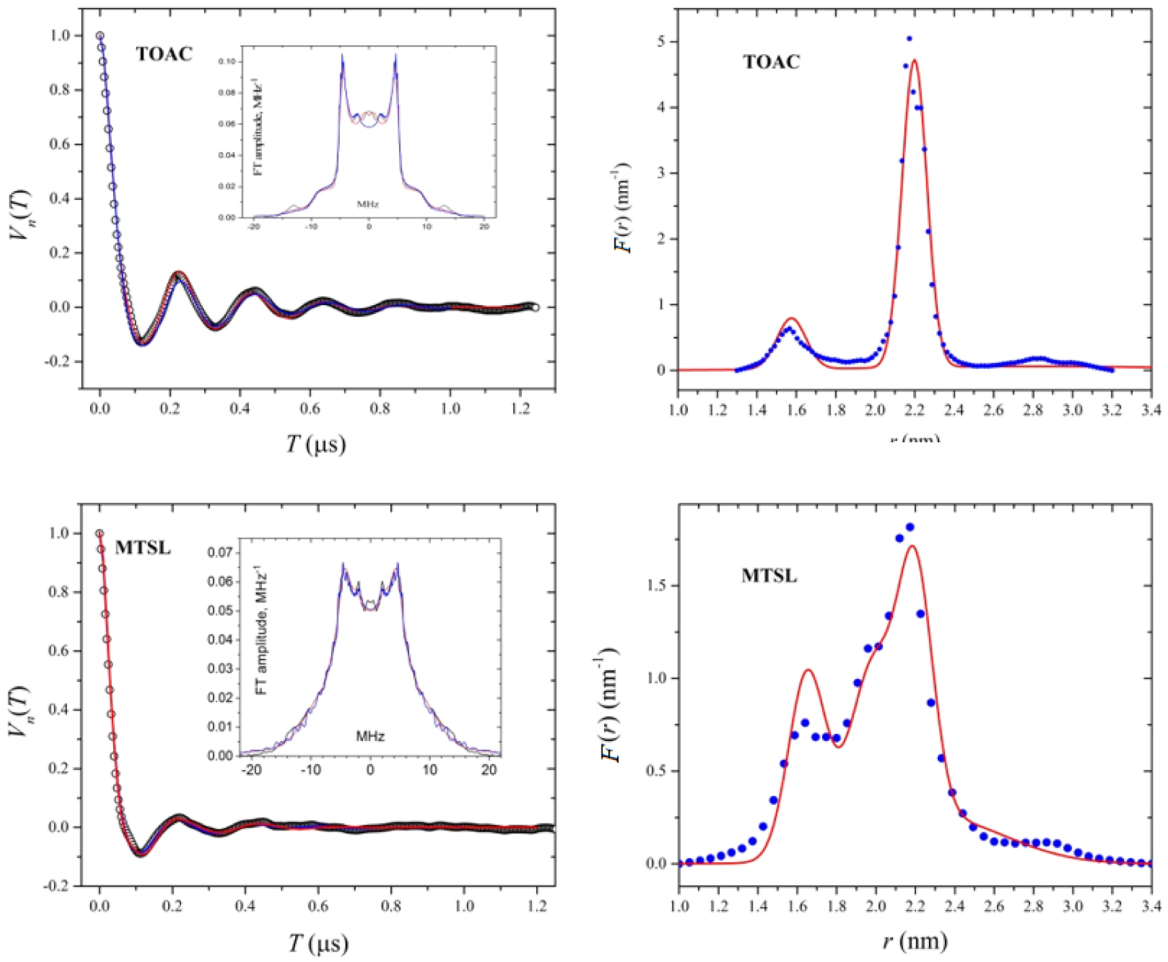

Figure 12. Left panels show the experimental normalized $V_n(T)$ time traces (black circles) averaged for different frequency offsets (see text), along with the best-fitted simulations employing the multi-Gaussian approximation (red line) and the distance discretization (blue line). In the insets, the related data in the frequency domain are illustrated. The right panels describe the obtained distance distributions employing the multi-Gaussian approximation (red curve) and the distance discretization (blue points). The peaks for $F(r)$ seen near 1.6 and 2.9 nm are artifacts induced by the residual proton- and deuteron-induced ESEEMs, respectively.

MTSL labels and therefore allow obtaining more precise data on distance distribution.

CONCLUSIONS

In this work, we have first studied, using FT-IR absorption, CD, and 2D NMR spectroscopies, the conformational tendencies of our terminally blocked 20-amino acid long, Aib-rich, unlabeled model peptide ruler (**I**) in 3D structure-supporting organic solvents and found it to be largely α-helical. Having thus established the almost complete rigidity of its backbone, we have then investigated by the same physicochemical techniques our two double-TOAC and double-Cys(MTSL) synthetic analogues (peptides **II** and **III**, respectively) and have found that they essentially maintain the conformation of their sequence precursor.

Finally, we have made the first detailed comparison between the flexibility of their nitroxide-bearing side chains by the use of CW-EPR and pulsed DEER (PELDOR) techniques on the *same* template peptide. It turns out clearly that the TOAC side-chain labels are remarkably more conformationally restricted than the corresponding MTSL labels, thus providing more precise data on side chain-to-side chain distance distribution. In summary, although the use of Cys(MTSL) would still remain the main DEER approach to determine this type of separation in any *large protein*,[75] the TOAC probe is certainly the best known so far to nitroxide electron spin labeling *much shorter*, helical *peptide-based molecules* accessible by chemical synthesis. In this context, it is relevant to note that soon after we submitted the original version of the present manuscript, a very important paper[76] was published reporting benchmark tests and guidelines for DEER experiments on *large proteins* characterized by nitroxide probes.

METHODS

Peptide Synthesis. The peptides were synthesized by the SPPS methodology according to the FastMoc protocol. The experimental conditions for the synthesis, purification, and characterization of the peptides are reported in the Supporting Information.

FT-IR Absorption. The FT-IR absorption spectra were recorded at room temperature using a PerkinElmer model 1720X FT-IR absorption instrument, nitrogen flushed with a sample shuttle device at 2 cm^{-1} nominal resolution, averaging 100 scans. Solvent (spectrograde deuterated chloroform, 99.8% *d*, Merck, Darmastadt, Germany) spectra were obtained under the same conditions. Cells with path lengths of 0.1 and 1.0 cm were used.

https://doi.org/10.1021/acsomega.1c06227
ACS Omega 2022, 7, 5154−5165

CD. The electronic CD curves in the far-UV region (below 260 nm) were obtained on a Jasco (Tokyo, Japan) model J-1500 spectropolarimeter with a fused quartz cell of 0.02 cm pathlength (Hellma, Mühlheim, Germany). The values are expressed in terms of $[\theta]_T$, the total molar ellipticity (deg × cm^2 × $dmol^{-1}$). Spectra were recorded at room temperature in water and in spectrograde MeOH (99.9% Acros Organics, Geel, Belgium) at 3×10^{-4} M peptide concentration. A second set of measurements was acquired in the near-UV and visible regions (300−600 nm) by the use of a 0.1 cm pathlength quartz cell and a 10^{-3} M peptide concentration in MeOH solution to investigate the contribution of the $n \rightarrow \pi^*$ transition of the nitroxyl chromophore in the absence of the competition with the amide (peptide) chromophores.[41,60,62]

NMR. The monodimensional and correlated spectroscopy (COSY)/total correlation spectroscopy (TOCSY)/NOESY 2D NMR spectra of the unlabeled peptide (**I**) were obtained at 298 K by the use of a Bruker AVANCE NEO-600 spectrometer from an about 1 mM concentration sample dissolved in approximately 700 μL of MeOH, d_3 solution. Suppression of the solvent signal was achieved by the use of an excitation sculpting program.[77] All homonuclear spectra were acquired by collecting 512 experiments, each one consisting of 64−80 scans and 2 K data points. The spin systems of the coded amino acid residues were identified using standard double-quantum filtered-COSY[78] and clean TOCSY[79] spectra. In the latter case, the spin-lock pulse sequence was 70 ms long. NOESY experiments were utilized for sequence-specific assignments.[65] To avoid the problem of spin diffusion, the build-up curve of the volumes of the NOE cross peaks as a function of the mixing time (50−500 ms) was obtained first (data not shown). The mixing time of the NOESY experiment used for interproton distance determination was 150 ms (i.e., in the linear part of the NOE build-up curve).

Modeling. Peptide modeling was designed by using PyMOL open source software, a molecular visualization program created by W. L. DeLano and commercialized by Schrödinger Inc.[80,81] Currently, PyMOL is one of the most utilized programs of this type in the area of macromolecules.

Electron Spin Resonance Measurements. The EPR experiments were carried out on two different X-band Bruker ELEXSYS E580 EPR spectrometers using either an ER 4118 X-MS-3 or ER 4118 X-MD-5 resonator in an Oxford Instruments CF-935 cryostat.

For measurements at room temperature, the samples were deaerated by a nitrogen flow and contained in 1 mm i.d. tubes. The spectra were acquired with a microwave (mw) power of 0.5 mW and a modulation amplitude of 1 G (modulation frequency of 100 kHz). Three scans were summed to improve the S/N ratio.

For low-temperature measurements, the peptides were dissolved in deuterated methanol (d_4) at a concentration of 200 μM, put in EPR tubes, and frozen quickly in liquid nitrogen to form a glass.

The cryostat was cooled by nitrogen flow to 80 K for pulse EPR measurements or to 100 K for CW-EPR measurements. In the CW-EPR measurements, the mw power was attenuated to −45 dB. The calibrated, nonattenuated output mw power of the Gunn diode was 200 mW. The modulation frequency and the modulation amplitude were 100 kHz and 0.1 mT, respectively. The time constant was 20.48 ms, and the conversion time was 40.96 ms.

The CW-EPR spectra were simulated by EasySpin software.[82]

The DEER experiments were performed with the three-pulse sequence $t_{pulse(\nu A)}-T-t_{pulse(\nu B)}-(\tau - T)-2t_{pulse(\nu A)}-\tau-$ echo, where the subscripts include notations for the detection (ν_A) and pumping (ν_B) mw frequencies. The time delay T for the pumping pulse was initially set to 200 ns prior to the first detection pulse and then scanned with a 4 ns time step. The frequency offset $\nu_A-\nu_B$ was chosen symmetrically around the absorption dip in the resonator and varied from 40 to 90 MHz and. The $t_{pulse(\nu A)}$ duration was 16 ns, the $t_{pulse(\nu_B)}$ duration was 28 ns. The amplitude of the pumping pulse was set to inverse the primary echo at the maximum of the echo-detected EPR spectrum. The amplitude of the detection pulse was chosen to provide the maximal echo signal. The time τ in the DEER measurements was 1600 ns. The noise amplitude on the normalized orientationally averaged DEER traces was 0.005−0.007. The DEER signal distortions upon the pumping pulse passage through the detecting pulses were corrected as already described.[83]

As the experimental DEER signal time-dependence is assumed to be a product of the intra- and intermolecular dipolar contributions, the former contribution was refined by approximating the latter by a stretched exponential function.[84] After elimination of this function, the resulting intramolecular part of the DEER time trace $V_{INTRA}(T)$ was normalized according to Milov et al.[85]

$$V_n(T) = \frac{V_{INTRA}(T) - V_{INTRA}(\infty)}{V_{INTRA}(0) - V_{INTRA}(\infty)} \quad (1)$$

The experimental modulation depth in the DEER experiments, $\lambda \equiv 1 - V_{intra}(\infty)$, was compared with the calculated one, λ_{calc}.[67] The comparison for both the TOAC- and Cys(MTSL)-labeled peptides is given in Supporting Information, Figure S6.

The experimental $V_n(T)$ time traces may be directly identified with the theoretical expression for the DEER signal time-dependence[85]

$$f(T) = \int_0^{\pi/2} \sin\theta d\theta \int_0^{\infty} \cos\left[\frac{g_1 g_{2\mu_B^2}}{h}\frac{1}{r^3}(1 - 3\cos^2\theta)T\right] F(r)dr \quad (2)$$

where $F(r)$ is related to the distance distribution function normalized in the way that $\int_0^{\infty} F(r)dr = 1$, g_1 and g_2 are the g-factors of the two spins, μ_B is the Bohr magneton, and θ is the angle between the external magnetic field and the vector connecting the spin pair. The experimental $V_n(T)$ time traces were cosine Fourier transformed.

The pair distance distribution function $F(r)$ was recovered by solving the integral eq 2 for which the equality $f(t) = V_n(T)$ was assumed. To avoid the instability of the solution because of the ill-posed nature of the problem,[68] two independent regularization approaches were used: (i) by the distance discretization with the Monte Carlo search of the solution[86] and (ii) by the multi-Gaussian Monte Carlo fitting.[87,88] Both approaches employ a fitting in the DEER frequency domain. The former approach is certainly model-free, while the latter produces smooth $F(r)$ functions possessing meanwhile a simple physical meaning.

https://doi.org/10.1021/acsomega.1c06227
ACS Omega 2022, 7, 5154−5165

■ ASSOCIATED CONTENT

Supporting Information

The Supporting Information is available free of charge at https://pubs.acs.org/doi/10.1021/acsomega.1c06227.

Description of the peptide synthesis, MS spectra and HPLC chromatograms of the different peptides, and additional IR absorption, CD, NMR, and EPR data (PDF)

■ AUTHOR INFORMATION

Corresponding Authors

Barbara Biondi − *Institute of Biomolecular Chemistry, Padova Unit, CNR, 35131 Padova, Italy;* orcid.org/0000-0003-2393-7333; Email: barbara.biondi@unipd.it

Victoria N. Syryamina − *Institute of Chemical Kinetics and Combustion, 630090 Novosibirsk, Russian Federation;* Email: v_syryamina@kinetics.nsc.ru

Authors

Gabriele Rocchio − *Department of Chemical Sciences, University of Padova, 35131 Padova, Italy*

Antonio Barbon − *Department of Chemical Sciences, University of Padova, 35131 Padova, Italy;* orcid.org/0000-0002-2009-5874

Fernando Formaggio − *Institute of Biomolecular Chemistry, Padova Unit, CNR, 35131 Padova, Italy; Department of Chemical Sciences, University of Padova, 35131 Padova, Italy*

Claudio Toniolo − *Institute of Biomolecular Chemistry, Padova Unit, CNR, 35131 Padova, Italy; Department of Chemical Sciences, University of Padova, 35131 Padova, Italy*

Jan Raap − *Leiden Institute of Chemistry, Gorlaeus Laboratories, Leiden University, 2300 RA Leiden, The Netherlands*

Sergei A. Dzuba − *Institute of Chemical Kinetics and Combustion, 630090 Novosibirsk, Russian Federation; Department of Physics, Novosibirsk State University, 630090 Novosibirsk, Russian Federation;* orcid.org/0000-0001-8880-6559

Complete contact information is available at: https://pubs.acs.org/10.1021/acsomega.1c06227

Notes

The authors declare no competing financial interest.

■ ACKNOWLEDGMENTS

V.N.S. and S.A.D. acknowledge financial support from the Russian Science Foundation, project # 21-13-00025. B.B. and F.F. are grateful to the Italian Ministry of Research (PRIN 2020 N. 2020833Y75) and to the University of Padova and Fresenius Kabi iPSUM (Uni-Impresa 2019 PEPTIND) for their financial support.

■ REFERENCES

(1) Milov, A. D.; Ponomarev, A. B.; Tsvetkov, Y. D. Electron-electron double resonance in electron spin echo: Model biradical systems and the sensitized photolysis of decalin. *Chem. Phys. Lett.* **1984**, *110*, 67−72.

(2) Milov, A. D.; Maryasov, A. G.; Tsvetkov, Y. D. Pulsed electron double resonance (PELDOR) and its applications in free-radicals research. *Appl. Magn. Reson.* **1998**, *15*, 107−143.

(3) Martin, R. E.; Pannier, M.; Diederich, F.; Gramlich, V.; Hubrich, M.; Spiess, H. W. Determination of end-to-end distances in a series of TEMPO diradicals of up to 2.8 nm length with a new four-pulse double electron electron resonance experiment. *Angew. Chem., Int. Ed.* **1998**, *37*, 2833−2837.

(4) Jeschke, G. DEER distance measurements on proteins. *Annu. Rev. Phys. Chem.* **2012**, *63*, 419−446.

(5) Schmidt, T.; Wälti, M. A.; Baber, J. L.; Hustedt, E. J.; Clore, G. M. Long distance measurements up to 160 Å in the GroEL tetradecamer using Q-Band DEER EPR spectroscopy. *Angew. Chem., Int. Ed.* **2016**, *55*, 15905−15909.

(6) Yang, Z.; Liu, Y.; Borbat, P.; Zweier, J. L.; Freed, J. H.; Hubbell, W. L. Pulsed ESR dipolar spectroscopy for distance measurements in immobilized spin labeled proteins in liquid solution. *J. Am. Chem. Soc.* **2012**, *134*, 9950−9952.

(7) Möbius, K.; Lubitz, W.; Savitsky, A. High-field EPR on membrane proteins − Crossing the gap to NMR. *Prog. Nucl. Magn. Reson. Spectrosc.* **2013**, *75*, 1−49.

(8) Borbat, P. P.; Freed, J. H. Pulse dipolar electron spin resonance: distance measurements. In *Structural Information from Spin-Labels and Intrinsic Paramagnetic Centres in the Biosciences*; Timmel, C. R., Harmer, J. R., Eds.; Springer: Berlin, 2013; pp 1−82.

(9) Schmidt, M. J.; Fedoseev, A.; Bücker, D.; Borbas, J.; Peter, C.; Drescher, M.; Summerer, D. EPR distance measurements in native proteins with genetically encoded spin labels. *ACS Chem. Biol.* **2015**, *10*, 2764−2771.

(10) Möbius, K.; Lubitz, W.; Cox, N.; Savitsky, A. Biomolecular EPR meets NMR at high magnetic fields. *Magnetochemistry* **2018**, *4*, 50.

(11) Sahu, I. D.; Lorigan, G. A. Site-directed spin labeling EPR for studying membrane proteins. *Biomed. Res. Int.* **2018**, *2018*, 3248289.

(12) Widder, P.; Berner, F.; Summerer, D.; Drescher, M. Double nitroxide labeling by copper-catalyzed azide−alkyne cycloadditions with noncanonical amino acids for electron paramagnetic resonance spectroscopy. *ACS Chem. Biol.* **2019**, *14*, 839−844.

(13) Columbus, L.; Kálai, T.; Jekö, J.; Hideg, K.; Hubbell, W. L. Molecular motion of spin labeled side chains in α-helices.Analysis by variation of side chain structure. *Biochemistry* **2001**, *40*, 3828−3846.

(14) Fleissner, M. R.; Cascio, D.; Hubbell, W. L. Structural origin of weakly ordered nitroxide motion in spin-labeled proteins. *Protein Sci.* **2009**, *18*, 893−908.

(15) Igarashi, R.; Sakai, T.; Hara, H.; Tenno, T.; Tanaka, T.; Tochio, H.; Shirakawa, M. Distance determination in proteins inside Xenopus laevis oocytes by double electron−electron resonance experiments. *J. Am. Chem. Soc.* **2010**, *132*, 8228−8229.

(16) Roser, P.; Schmidt, M. J.; Drescher, M.; Summerer, D. Site-directed spin labeling of proteins for distance measurements in vitro and in cells. *Org. Biomol. Chem.* **2016**, *14*, 5468−5476.

(17) Lawless, M. J.; Shimshi, A.; Cunningham, T. F.; Kinde, M. N.; Tang, P.; Saxena, S. Analysis of nitroxide-based distance measurements in cell extracts and in cells by pulsed ESR spectroscopy. *ChemPhysChem* **2017**, *18*, 1653−1660.

(18) Yang, C.; Lo, W.-L.; Kuo, Y.-H.; Sang, J. C.; Lee, C.-Y.; Chiang, Y.-W.; Chen, R. P.-Y. Revealing structural changes of prion protein during conversion from α-helical monomer to β-oligomers by means of ESR and nanochannel encapsulation. *ACS Chem. Biol.* **2015**, *10*, 493−501.

(19) Kuznetsov, N. A.; Milov, A. D.; Isaev, N. P.; Vorobjev, Y. N.; Koval, V. V.; Dzuba, S. A.; Fedorova, O. S.; Tsvetkov, Y. D. PELDOR analysis of enzyme-induced structural changes in damaged DNA duplexes. *Mol. BioSyst.* **2011**, *7*, 2670−2680.

(20) Kuznetsov, N. A.; Milov, A. D.; Koval, V. V.; Samoilova, R. I.; Grishin, Y. A.; Knorre, D. G.; Tsvetkov, Y. D.; Fedorova, O. S.; Dzuba, S. A. PELDOR study of conformations of double-spin-labeled single- and double-stranded DNA with non-nucleotide inserts. *Phys. Chem. Chem. Phys.* **2009**, *11*, 6826−6832.

(21) Sameach, H.; Ruthstein, S. EPR distance measurements as a tool to characterize protein-DNA interactions. *Isr. J. Chem.* **2019**, *59*, 980−989.

(22) Milov, A. D.; Tsvetkov, Y. D.; Formaggio, F.; Crisma, M.; Toniolo, C.; Raap, J. Self-assembling properties of membrane-modifying peptides studied by PELDOR and CW-ESR spectroscopies. *J. Am. Chem. Soc.* **2000**, *122*, 3843−3848.
(23) Milov, A. D.; Tsvetkov, Y. D.; Formaggio, F.; Crisma, M.; Toniolo, C.; Raap, J. The secondary structure of a membrane-modifying peptide in a supramolecular assembly studied by PELDOR and CW-ESR spectroscopies. *J. Am. Chem. Soc.* **2001**, *123*, 3784−3789.
(24) Salnikov, E. S.; Erilov, D. A.; Milov, A. D.; Tsvetkov, Y. D.; Peggion, C.; Formaggio, F.; Toniolo, C.; Raap, J.; Dzuba, S. A. Location and aggregation of the spin-labeled peptide trichogin GA IV in a phospholipid membrane as revealed by pulsed EPR. *Biophys. J.* **2006**, *91*, 1532−1540.
(25) Milov, A. D.; Samoilova, R. I.; Tsvetkov, Y. D.; Formaggio, F.; Toniolo, C.; Raap, J. Self-aggregation of spin-labeled alamethicin in ePC vesicles studied by pulsed electron−electron double resonance. *J. Am. Chem. Soc.* **2007**, *129*, 9260−9261.
(26) Syryamina, V. N.; De Zotti, M.; Toniolo, C.; Formaggio, F.; Dzuba, S. A. Alamethicin self-assembling in lipid membranes: concentration dependence from pulsed EPR of spin labels. *PhysChemChemPhys* **2018**, *20*, 3592−3601.
(27) Afanasyeva, E. F.; Syryamina, V. N.; De Zotti, M.; Formaggio, F.; Toniolo, C.; Dzuba, S. A. Peptide antibiotic trichogin in model membranes: Self-association and capture of fatty acids. *Biochim. Biophys. Acta, Biomembr.* **2019**, *1861*, 524−531.
(28) Golysheva, E. A.; Samoilova, R. I.; De Zotti, M.; Formaggio, F.; Gobbo, M.; Dzuba, S. A. ESE-detected molecular motions of spin-labeled molecules on a solid inorganic surface: motional models and onset temperatures. *Appl. Magn. Reson.* **2020**, *51*, 1019−1029.
(29) Syryamina, V. N.; Samoilova, R. I.; Tsvetkov, Y. D.; Ischenko, A. V.; De Zotti, M.; Gobbo, M.; Toniolo, C.; Formaggio, F.; Dzuba, S. A. Peptides on the surface: spin-label EPR and PELDOR study of adsorption of the antimicrobial peptides trichogin GA IV and ampullosporin A on the silica nanoparticles. *Appl. Magn. Reson.* **2016**, *47*, 309−320.
(30) Mezzina, E.; Manoni, R.; Romano, F.; Lucarini, M. Spin-labelling of host-guest assemblies with nitroxide radicals. *Asian J. Org. Chem.* **2015**, *4*, 296−310.
(31) Li, H.; Pan, Y.; Yang, Z.; Rao, J.; Chen, B. Emerging applications of site-directed spin labeling electron paramagnetic resonance (SDSL-EPR) to study food protein structure, dynamics, and interaction. *Trends Food Sci. Technol.* **2021**, *109*, 37−50.
(32) Miao, Q.; Zurlo, E.; Bruin, D.; Wondergem, J. A. J.; Timmer, M.; Blok, A.; Heinrich, D.; Overhand, M.; Huber, M.; Ubbink, M. A two-armed probe for in-cell DEER measurements on proteins. *Chem. - Eur. J.* **2020**, *26*, 17128−17133.
(33) Cunningham, T. F.; Putterman, M. R.; Desai, A.; Horne, W. S.; Saxena, S. The double-histidine Cu^{2+}-binding motif: a highly rigid, site-specific spin probe for electron spin resonance distance measurements. *Angew. Chem., Int. Ed.* **2015**, *54*, 6330−6334.
(34) Owenius, R.; Eaton, G. R.; Eaton, S. S. Frequency (250MHz to 9.2GHz) and viscosity dependence of electron spin relaxation of triarylmethyl radicals at room temperature. *J. Magn. Reson.* **2005**, *172*, 168−175.
(35) Ketter, S.; Gopinath, A.; Rogozhnikova, O.; Trukhin, D.; Tormyshev, V. M.; Bagryanskaya, E. G.; Joseph, B. In situ labeling and distance measurements of membrane proteins in E. coli using Finland and OX063 trityl labels. *Chem.—Eur. J.* **2021**, *27*, 2299−2304.
(36) Rassat, A.; Rey, P. Preparation d'amino acides radicalaires et de leurs sels complexes. *Bull. Soc. Chim. Fr.* **1967**, *3*, 815−818.
(37) Nakaie, C. R.; Schreier, S.; Paiva, A. C. M. Synthesis and properties of spin-labeled angiotensin derivatives. *Biochim. Biophys. Acta* **1983**, *742*, 63−71.
(38) Toniolo, C.; Valente, E.; Formaggio, F.; Crisma, M.; Pilloni, G.; Corvaja, C.; Toffoletti, A.; Martinez, G. V.; Hanson, M. P.; Millhauser, G. L.; George, C.; Flippen-Anderson, J. L. Synthesis and conformational studies of peptides containing TOAC, a spin-labelled $C^{\alpha,\alpha}$-disubstituted glycine. *J. Pept. Sci.* **1995**, *1*, 45−57.
(39) Crisma, M.; Deschamps, J. R.; George, C.; Flippen-Anderson, J. L.; Kaptein, B.; Broxterman, Q. B.; Moretto, A.; Oancea, S.; Jost, M.; Formaggio, F.; Toniolo, C. A topographically and conformationally constrained, spin-labeled, α-amino acid. Crystallographic characterization in peptides. *J. Pept. Res.* **2005**, *65*, 564−579.
(40) van Eps, N.; Anderson, L. L.; Kisselev, O. G.; Baranski, T. J.; Hubbell, W. L.; Marshall, G. R. Electron paramagnetic resonance studies of functionally active, nitroxide spin-labeled peptide analogues of the C-terminus of a G-protein α subunit. *Biochemistry* **2010**, *49*, 6877−6886.
(41) Schreier, S.; Bozelli, J. C.; Marín, N.; Vieira, R. F. F.; Nakaie, C. R. The spin label amino acid TOAC and its uses in studies of peptides. Chemical, physicochemical, spectroscopic, and conformational aspects. *Biophys. Rev.* **2012**, *4*, 45−66.
(42) Berliner, L. J.; Grunwald, J.; Hankovszky, H. O.; Hideg, K. A novel reversible thiol-specific spin label: Papain active site labeling and inhibition. *Anal. Biochem.* **1982**, *119*, 450−455.
(43) Stoller, S.; Sicoli, G.; Baranova, T. Y.; Bennati, M.; Diederichsen, U. TOPP: a novel nitroxide-labeled amino acid for EPR distance measurements. *Angew. Chem., Int. Ed.* **2011**, *50*, 9743−9746.
(44) Warshaviak, D. T.; Serbulea, L.; Houk, K. N.; Hubbell, W. L. Conformational analysis of a nitroxide side chain in an α-helix with density functional theory. *J. Phys. Chem. B* **2011**, *115*, 397−405.
(45) Zurlo, E.; Gorroño Bikandi, I.; Meeuwenoord, N. J.; Filippov, D. V.; Huber, M. Tracking amyloid oligomerization with monomer resolution using a 13-amino acid peptide with a backbone-fixed spin label. *Phys. Chem. Chem. Phys.* **2019**, *21*, 25187−25195.
(46) Smythe, M. L.; Nakaie, C. R.; Marshall, G. R. α-Helical versus 3_{10}-helical conformation of alanine-based peptides in aqueous solution: an electron spin resonance investigation. *J. Am. Chem. Soc.* **1995**, *117*, 10555−10562.
(47) Hanson, P.; Millhauser, G.; Formaggio, F.; Crisma, M.; Toniolo, C. ESR characterization of hexameric, helical peptides usng double TOAC spin labeling. *J. Am. Chem. Soc.* **1996**, *118*, 7618−7625.
(48) Golysheva, E. A.; Boyle, A. L.; Biondi, B.; Ruzza, P.; Kros, A.; Raap, J.; Toniolo, C.; Formaggio, F.; Dzuba, S. A. Probing the E/K peptide coiled-coil assembly by double electron-electron resonance and circular dichroism. *Biochemistry* **2021**, *60*, 19−30.
(49) Fasman, G. D. Factors responsible for conformational stability. In *Poly-α-Amino acids: Protein Models for Conformational Studies*; Fasman, G. D., Ed.; Dekker: N. Y., 1967; pp 499−605.
(50) Karle, I. L.; Balaram, P. Structural characteristics of α-helical peptide molecules containing Aib residues. *Biochemistry* **1990**, *29*, 6747−6756.
(51) Toniolo, C.; Crisma, M.; Formaggio, F.; Peggion, C. Control of peptide conformation by the Thorpe-Ingold effect (C^{α}-tetrasubstitution). *Biopolymers* **2001**, *60*, 396−419.
(52) Carpino, L. A. 1-Hydroxy-7-azabenzotriazole. An efficient peptide coupling additive. *J. Am. Chem. Soc.* **1993**, *115*, 4397−4398.
(53) Zotti, M.; Biondi, B.; Peggion, C.; Formaggio, F.; Park, Y.; Hahm, K.-S.; Toniolo, C. Trichogin GA IV: a versatile template for the synthesis of novel peptaibiotics. *Org. Biomol. Chem.* **2012**, *10*, 1285−1299.
(54) Marchetto, R.; Schreier, S.; Nakaie, C. R. A novel spin-labeled amino-acid derivative for use in peptide-synthesis - (9-Fluorenylmethyloxycarbonyl)-2,2,6,6-tetramethylpiperidine-N-oxyl-4-amino-4-carboxylic acid. *J. Am. Chem. Soc.* **1993**, *115*, 11042−11043.
(55) Yasui, S. C.; Keiderling, T. A.; Formaggio, F.; Bonora, G. M.; Toniolo, C. Vibrational circular dichroism of polypeptides. 9. A study of chain length dependence for 3_{10}-helix formation in solution. *J. Am. Chem. Soc.* **1986**, *108*, 4988−4993.
(56) Kennedy, D. F.; Crisma, M.; Toniolo, C.; Chapman, D. Studies of peptides forming 3_{10}- and α-helices and β-bend ribbon structures in organic solution and in model biomembranes by Fourier transform infrared spectroscopy. *Biochemistry* **1991**, *30*, 6541−6548.
(57) Toniolo, C.; Crisma, M.; Formaggio, F. TOAC, a nitroxide spin-labeled, achiral C^{α}-tetrasubstituted α-amino acid, is an excellent

https://doi.org/10.1021/acsomega.1c06227
ACS Omega 2022, 7, 5154−5165

tool in materials science and biochemistry. *Biopolymers* **1998**, *47*, 153−158.
(58) Manning, M. C.; Woody, R. W. Theoretical CD studies of polypeptide helices. Examination of important electronic and geometric factors. *Biopolymers* **1991**, *31*, 569−586.
(59) Toniolo, C.; Polese, A.; Formaggio, F.; Crisma, M.; Kamphuis, J. Circular dichroism spectrum of a peptide 3_{10}-helix. *J. Am. Chem. Soc.* **1996**, *118*, 2744−2745.
(60) Bui, T. T. T.; Formaggio, F.; Crisma, M.; Monaco, V.; Toniolo, C.; Hussain, R.; Siligardi, G. TOAC: a useful C^{α}-tetrasubstituted α-aminoacid for peptide conformational analysis by CD spectroscopy in the visible region .Part I. *J. Chem .Soc .,Perkin Trans .* **2000**, *2*, 1043−1046.
(61) Moretto, A.; Formaggio, F.; Kaptein, B.; Broxterman, Q. B.; Wu, L.; Keiderling, T. A.; Toniolo, C. First homo-peptides undergoing a reversible 3_{10}-helix/α-helix transition. Critical main-chain length. *Biopolymers (Pept. Sci.)* **2008**, *90*, 567−574.
(62) Polese, A.; Anderson, D. J.; Millhauser, G.; Formaggio, F.; Crisma, M.; Marchiori, F.; Toniolo, C. First interchain peptide interaction detected by ESR in fully synthetic, template-assisted, two-helix bundles. *J. Am. Chem. Soc.* **1999**, *121*, 11071−11078.
(63) Concilio, M. G.; Fielding, A. J.; Bayliss, R.; Burgess, S. G. Density functional theory studies of MTSL nitroxide side chain conformations attached to an activation loop. *Theor. Chem. Acc.* **2016**, *135*, 97.
(64) Jeschke, G. Conformational dynamics and distribution of nitroxide spin labels. *Prog. Nucl. Magn. Reson. Spectrosc.* **2013**, *72*, 42−60.
(65) Wüthrich, K. *NMR of Proteins and Nucleic Acids*; Wiley: N. Y., 1986.
(66) Tonlolo, C.; Benedetti, E. The polypeptide 3_{10}-helix. *Trends Biochem. Sci.* **1991**, *16*, 350−353.
(67) Milov, A. D.; Shirov, M. D. Application of ELDOR in electron-spin echo for paramagnetic center space distribution in solids. *Fiz. Tverd. Tela* **1981**, *23*, 975−982.
(68) Jeschke, G.; Chechik, V.; Ionita, P.; Godt, A.; Zimmermann, H.; Banham, J.; Timmel, C. R.; Hilger, D.; Jung, H. DEER analysis 2006: a comprehensive software package for analyzing pulsed ELDOR data. *Appl. Magn. Reson.* **2006**, *30*, 473−498.
(69) Polyhach, Y.; Godt, A.; Bauer, C.; Jeschke, G. Spin pair geometry revealed by high-field DEER in the presence of conformational distributions. *J. Magn. Reson.* **2007**, *185*, 118−129.
(70) Schiemann, O.; Cekan, P.; Margraf, D.; Prisner, T. F.; Sigurdsson, S. T. Relative orientation of rigid nitroxides by PELDOR: beyond distance measurements in nucleic acids. *Angew. Chem., Int. Ed.* **2009**, *48*, 3292−3295.
(71) Abé, C.; Klose, D.; Dietrich, F.; Ziegler, W. H.; Polyhach, Y.; Jeschke, G.; Steinhoff, H.-J. Orientation selective DEER measurements on vinculin tail at X-band frequencies reveal spin label orientations. *J. Magn. Reson.* **2012**, *216*, 53−61.
(72) Abdullin, D.; Hagelueken, G.; Hunter, R. I.; Smith, G. M.; Schiemann, O. Geometric model-based fitting algorithm for orientation-selective PELDOR data. *Mol. Phys.* **2015**, *113*, 544−560.
(73) Baber, J. L.; Louis, J. M.; Clore, G. M. Dependence of distance distributions derived from double electron−electron resonance pulsed EPR spectroscopy on pulse-sequence time. *Angew. Chem., Int. Ed.* **2015**, *54*, 5336−5339.
(74) Schmidt, T.; Clore, G. M. T_m filtering by ^{1}H-methyl labeling in a deuterated protein for pulsed double electron−electron resonance EPR. *Chem. Commun.* **2020**, *56*, 10890−10893.
(75) Balo, A. R.; Feyrer, H.; Ernst, O. P. Toward precise interpretation of DEER-based distance distributions: insights from structural characterization of V1 spin-labeled side chains. *Biochemistry* **2016**, *55*, 5256−5263.
(76) Schiemann, O.; Heubach, C. A.; Abdullin, D.; Ackermann, K.; Azarkh, M.; Bagryanskaya, E. G.; Drescher, M.; Endeward, B.; Freed, J. H.; Galazzo, L.; Goldfarb, D.; Hett, T.; Esteban Hofer, L.; Fábregas Ibáñez, L.; Hustedt, E. J.; Kucher, S.; Kuprov, I.; Lovett, J. E.; Meyer, A.; Ruthstein, S.; Saxena, S.; Stoll, S.; Timmel, C. R.; Di Valentin, M.; Mchaourab, H. S.; Prisner, T. F.; Bode, B. E.; Bordignon, E.; Bennati, M.; Jeschke, G. Benchmark test and guidelines for DEER/PELDOR experiments on nitroxide-labeled biomolecules. *J. Am. Chem. Soc.* **2021**, *143*, 17875−17890.
(77) Hwang, T. L.; Shaka, A. J. Water suppression that works. Excitation sculpting using arbitrary wave-forms and pulsed-field gradients. *J. Magn. Reson., Ser. A* **1995**, *112*, 275−279.
(78) Rance, M.; Sørensen, O. W.; Bodenhausen, G.; Wagner, G.; Ernst, R. R.; Wüthrich, K. Improved spectral resolution in COSY ^{1}H NMR spectra of proteins via double quantum filtering. *Biochem. Biophys. Res. Commun.* **1983**, *117*, 479−485.
(79) Griesinger, C.; Otting, G.; Wüthrich, K.; Ernst, R. R. Clean TOCSY for proton spin system identification in macromolecules. *J. Am. Chem. Soc.* **1988**, *110*, 7870−7872.
(80) Baugh, E. H.; Lyskov, S.; Weitzner, B. D.; Gray, J. J. Real-time PyMOL visualization for Rosetta and PyRosetta. *PLoS One* **2011**, *6*, No. e21931.
(81) Bramucci, E.; Paiardini, A.; Bossa, F.; Pascarella, S. PyMod: sequence similarity searches, multiple sequence-structure alignments, and homology modeling within PyMOL. *BMC Bioinf.* **2012**, *13*, S2.
(82) Stoll, S.; Schweiger, A. EasySpin, a comprehensive software package for spectral simulation and analysis in EPR. *J. Magn. Reson.* **2006**, *178*, 42−55.
(83) Milov, A. D.; Grishin, Y. A.; Dzuba, S. A.; Tsvetkov, Y. D. Effect of pumping pulse duration on echo signal amplitude in four-pulse PELDOR. *Appl. Magn. Reson.* **2011**, *41*, 59−67.
(84) Kattnig, D. R.; Reichenwallner, J.; Hinderberger, D. Modeling excluded volume effects for the faithful description of the background signal in double electron−electron resonance. *J. Phys. Chem. B* **2013**, *117*, 16542−16557.
(85) Milov, A. D.; Tsvetkov, Y. D.; Maryasov, A. G.; Gobbo, M.; Prinzivalli, C.; De Zotti, M.; Formaggio, F.; Toniolo, C. Conformational properties of the spin-labeled tylopeptin B and heptaibin peptaibiotics based on PELDOR spectroscopy data. *Appl. Magn. Reson.* **2013**, *44*, 495−508.
(86) Dzuba, S. A. The determination of pair-distance distribution by double electron-electron resonance: regularization by the length of distance discretization with Monte Carlo calculations. *J. Magn. Reson.* **2016**, *269*, 113−119.
(87) Matveeva, A. G.; Yushkova, Y. V.; Morozov, S. V.; Grygor'ev, I. A.; Dzuba, S. A. Multi-gaussian Monte Carlo analysis of PELDOR data in the frequency domain. *Z. Phys. Chem.* **2017**, *231*, 671−688.
(88) Kuznetsova, A. A.; Matveeva, A. G.; Milov, A. D.; Vorobjev, Y. N.; Dzuba, S. A.; Fedorova, O. S.; Kuznetsov, N. A. Substrate specificity of human apurinic/apyrimidinic endonuclease APE1 in the nucleotide incision repair pathway. *Nucleic Acids Res.* **2018**, *46*, 11454−11465.

https://doi.org/10.1021/acsomega.1c06227
ACS Omega 2022, 7, 5154−5165